(4)

Technical Document 1963
December 1990

Photoresponse Studies of Ion-Damaged Germanium for Optoelectronic Switch Applications

S. D. Russell

NAVAL OCEAN SYSTEMS CENTER

San Diego, California 92152-5000

J. D. FONTANA, CAPT, USN
Commander

H. R. TALKINGTON, Acting
Technical Director

ADMINISTRATIVE INFORMATION

This research was performed under the Optoelectronic/Time Division Multiplexing (OE/TDM) Project from June to October 1986 under the direction of Dr. D. J. Albares, NOSC Code 553. During this time, the author was in NOSC's New Professional (NP) Program, Code 1431.

This work was performed for the Defense Advanced Projects Agency (DARPA), 1400 Wilson Boulevard, Arlington, VA 22209, under program element 0602301E.

Released by
G. A. Garcia, Head
Research and Technology
Branch

Under authority of
H. E. Rast, Head
Solid State Electronics
Division

ACKNOWLEDGMENTS

The author wishes to thank individuals for their helpful discussions during the period covered by this report. These acknowledgments include Dr. D. J. Albares, Dr. R. E. Reedy, and Dr. G. A. Garcia (NOSC); Dr. C. T. Chang (SDSU); and Dr. S. S. Lau (UCSD). Particular appreciation is given to Dr. T. Sigmon and J. Abelson (Stanford University) for the training and use of the RBS facilities.

MA

SUMMARY

OBJECTIVE

Examine the effect of crystalline damage on photoresponse of elemental germanium as a proposed method to decrease the photocurrent decay time for high-speed optoelectronic (OE) switch applications.

RESULTS

Ion implantation was used to create predetermined defect densities in germanium. Characterization of crystallinity used x-ray diffraction, spreading resistance profilometry (SRP), and Rutherford backscattering spectroscopy (RBS) techniques. Ion-damaged germanium shows a significant decrease in photoresponsivity with implant dose, particularly with doses exceeding the critical amorphizing dose ($D_c \approx 1 \times 10^{14} cm^{-2}$).

CONCLUSION/RECOMMENDATIONS

RBS proved to be the most valuable technique in quantifying the degree of damage. The decrease in photoresponsivity with increasing implant dose requires minimizing the degree of damage to optimize the OE switch photoresponse.

Solutions to contact problems need to be developed before OE switches can be fabricated on germanium. Only then can the optimal implant dose required for satisfactory switching times be determined.

Focused ion beams or laser processing techniques may be incorporated for spatial control over the damaged area now lacking in the technique. Advanced alloys and structures are also suggested as viable alternatives for OE switches.

CONTENTS

1. BACKGROUND 1

2. INTRODUCTION 2

3. EXPERIMENTAL 2

4. RESULTS 3

   4.1 Ion Implantation and RBS Analysis 3
   4.2 Spreading Resistance Profilometry 5
   4.3 X-Ray Diffraction 7
   4.4 Photoresponse Measurements 7

5. CONCLUSION 8

   5.1 Summary 8
   5.2 Proposed Switching Measurements 8
   5.3 Other Directions 9

6. GLOSSARY 10

7. REFERENCES 10

FIGURES

1. RBS spectra of ion-damaged germanium 4

2. Damage dependence on Ar^+ implantation dose in Ge 5

3. Damage concentration versus depth 6

4. Spreading resistance profile 6

5. Photoresponse versus laser power for unimplanted Ge 7

6. Photoresponse versus laser power from undamaged, moderately damaged (1×10^{13} Ar^+/cm^2), heavily damaged (5×10^{14} Ar^+/cm^2), and amorphous Ge 8

1. BACKGROUND

Major investments have been made by both the Department of Defense and private industry to advance the state of very-large-scale integration of electronics (VLSI). Development goals include integrated circuits with submicrometer device dimensions and up to 100,000 logic gates per chip. Efforts to meet these capabilities suffer from inherent limitations due to interconnections. Off-chip data transmission from VLSI chips require output buffer amplifiers to drive the capacitance of the bonding pads and wires attached to the chip-carrier conductors. Charging this capacitive load requires large drive transistors and limits output data rates to about 10 Mb/s. Consequently, digital words are transmitted in parallel both on and off VLSI chips. This approach results in a large number of interconnections that reduces reliability, uses significant chip area, and can consume a large percentage of the chip-power budget. Since on-chip capacitive loads are much smaller than output loads, VLSI on-chip devices operate at speeds 10–100 times faster than output data rates. Therefore, the output stages place significant limitations on systems architecture. New developments in down-scaling devices under the very-high-speed integrated circuits (VHSIC) program will increase device speed and density thus magnifying the interconnect problems.

A proposed solution to the above interconnect problems by Albares and Reedy[1] is through the implementation of optoelectronic/ time division multiplexing (OE/TDM). The serialization of output data via OE/TDM decreases the number of output connections, thereby improving reliability and diminishing the area needed for interconnections. The use of optoelectronic (OE) switches triggered via modulation of an off-chip laser diode results in little dissipation of optical and electrical energy on-chip. Multiplexing is achieved using optical fibers of different lengths to couple the diode laser to the OE switches. The optical pulse closes the OE switches sequentially at proper time delays thereby serializing the output data.

The optoelectronic switch used in the OE/ TDM technique is an electrical transmission line made up of a conductive microstrip line with a gap filled by a high-resistivity photoconductor. When light strikes the photoconductor, electron-hole pairs are generated lowering the gap resistance by several decades and thus closing the switch.[2] Early phases of development have demonstrated the feasibility of the OE/TDM technique using four gallium arsenide (GaAs) OE switches.[3]

Due to the demonstration of the OE/TDM technique as a potential solution to the VLSI/ VHSIC interconnect problems, concurrent research is being performed on the optimization of the OE switches. Several factors need to be considered in the optimal implementation of OE switches to TDM:

(a) optimal coupling between the fiber optics and the OE switches,

(b) development of materials with sufficiently fast response time and photosensitivity, and

(c) integrability of OE switch material into present silicon device manufacturing technology.

The first condition results from minimizing the energy demand per switch driven by the laser diode. This would trigger a large number of OE switches using a minimum number of laser diodes (anticipating future applications with ≥64-bit words). Operation at a wavelength of minimum attenuation in the optical fiber (1.55 μm) is planned, along with optimizing the OE switch interelectrode gap geometry. Recent experiments at 0.85 μm using metal-semiconductor metal (MSM) switches fabricated in InP with a variety of gap geometries have have demonstrated 2.5 Gb/s and an 8:1 multiplexing ratio.[4] Due to the large bandgaps of the materials most often used as OE switches (e.g., Si, GaAs, InP), intrinsic photoexcitation of carriers at 1.55 μm is not possible.[2,5] Germanium (Ge), with a bandgap of 0.67 eV (at 300 K),[5,6] has therefore been proposed as a candidate suitable for these OE switches. Particular interest

arises due to its miscibility with silicon and its small lattice mismatch with GaAs, thereby making it a unique material for potential device manufacturing requirements demanded by the third condition above. Research into the photoconductive response and sensitivity of germanium OE switches is therefore desirable in the development of OE/TDM.

2. INTRODUCTION

In light of the potential of germanium OE switches for OE/TDM applications, preliminary research into its photoresponse was performed. Recent investigations of semiconductor OE switches have demonstrated their operation in the picosecond (ps) regime.[7-10] A major thrust of that research has been concerned with decreasing the switching times of these devices,[11-15] the significance in terms of OE/TDM is the transmittal of higher data rates off-chip. The switching time (i.e., the photocurrent decay time) is determined by the recombination rate of the photoexcited electron-hole pairs. The dynamic processes involved in recombination have been well studied[16-22] and have resulted in two basic approaches used to achieve fast photocurrent decay times:

(a) compensating impurities such as Fe in InP[23] or Cr in GaAs[24] and

(b) defects as found in polycrystalline, amorphous, and radiation-damaged semiconductors.

Both approaches introduce energy levels in the bandgap that act as recombination centers and reduce the minority carrier lifetime. Amorphous silicon (a-Si) films prepared by chemical vapor deposition (CVD) or evaporation, exhibit recombination times on the order of 10 ps.[11,14,15] Switches made of polycrystalline germanium (p-Ge) films on sapphire have demonstrated recombination times less than 50 ps.[13] Controlling the defect concentration by varying ion-implantation doses has been shown effective in silicon-on-sapphire (SOS) by increasing the recombination rate with increasing defects.[8,10,25] In addition, the ion-damage technique has the favorable characteristic of higher carrier mobilities with similar recombination times when compared to other damage techniques,[8] implying greater photoresponsivity.

We report here our study of the photoresponse of ion-implanted germanium. The objective of this study was to examine the effect of crystalline damage on the photoresponse of elemental germanium as a proposed method to decrease the photocurrent decay time. The ion-implantation technique enabled the preparation of a predetermined defect density into the sample thus providing a range of crystallinity for study. The results show a significant decrease in photoresponsivity with implant dose, particularly with doses $\geq D_c$ (the critical amorphising dose). Proposal for continued research on photoconductive switching time and photoconductive materials and structures is given.

3. EXPERIMENTAL

Samples were constructed from (100) p-type germanium wafers, 2-inch diameter and nominally 15 mils thick. The wafers, having a resistivity in the range 1 to 10 Ω-cm, were mechanically polished on one side. A scanned beam of argon ions ($^{40}Ar^{+}$) at ambient temperature was used to implant the wafers with doses in the range 1×10^{13} ions/cm^2 (at 20 μA beam current) to 1×10^{16} ions/cm^2 (at 100 μA) at a 7° tilt to the surface normal. No surface damage was observed with a Nomarski microscope indicating minimal sample heating due to the scanning implant technique. The wafers were subsequently diced into 0.7 cm^2 samples for analysis. Characterization of the samples was performed using the techniques described below.

Both random and channeled Rutherford backscattering (RBS) spectra were obtained with a 2.2 MeV $^{4}He^{+}$ beam using the accelerator at Stanford University. Channeling measurements were oriented with the (100) crystal axis within 0.1° of the incident beam, while the random spectrum was obtained while rotating the sample at a 6.0° tilt to the incident beam. In both cases, the detector was mounted at 170° with respect to the beam, with an energy to channel

number conversion of 3.5 keV/ch. Using the published stopping cross-sections,[26] the depth conversion is 58.7 Å/ch or 16.8 Å/keV.

Spreading resistance as a function of depth was obtained on bevel-polished samples using Solid State Measurements, SSM-130 spreading resistance probe system. Depth resolution of -0.02 μm was obtained.

A General Electric X-ray generator with copper target emitting $k_{\alpha 1}$, $k_{\alpha 2}$, k_{β} and Bremstrahlung radiation was used to obtain Laue photos of the diffraction pattern. Samples were mounted 1.5 inches from sample to film (Polaroid type 57, 3000 ASA) to record the transmitted Bragg peaks. At 40 kV and 20 mA, exposures of -29 hours were required.

Photoresponse measurements were performed using a two-point surface probe technique, with percent changes in resistivity under photoexcitation recorded. Photoexcitation was accomplished with the attenuated beam of a Coherent model CR-18 Supergraphite argon ion laser. Operating in continuous wave (cw) mode at 5145 Å with light regulation, long-term stability was better than 1%, with noise and ripple < 0.5% rms. The circular beam has a diameter of 1.90 mm (at $1/e^2$ points) and a beam divergence of 0.43 mrad.[27] Prior to measurements, samples were cleaned using a degreasing (60% methanol-40% acetone) solution and mild etch (30% H_2O_2),[28] then rinsed in distilled water.

4. RESULTS

4.1 ION IMPLANTATION AND RBS ANALYSIS

To use the predetermining capability of the ion-implantation technique for defect formation, the critical dose required to yield an amorphous layer in the absence of vacancy out-diffusion was calculated. This is given by

$$D_c = \frac{E_d n_t}{\left(\frac{dE}{dx}\right)} \text{cm}^{-2} \qquad (1)$$

where D_c is the critical dose, E_d is the effective energy to displace a target lattice atom (in eV), n_t is the density of target atoms (cm^{-3}), and dE/dx is the energy-independent nuclear energy loss per unit path length. This energy loss factor can be approximated to yield the Nielson equation.[29,30]

$$\left(\frac{dE}{dx}\right) \simeq 7 \times 10^8 \rho_t Z_i^{2/3} \frac{M_i}{(M_i + M_t)} \text{ eV/cm} \qquad (2)$$

with the ion and target masses denoted by M_i and M_t respectively, ρ_t is the target density (in grams/cm^2) and Z_i is the atomic number of the implanted ion. E_d is taken as 25 eV, which is twice the estimate of the threshold energy required to break all bonds on germanium. This yields a critical dose $D_c = 1.2 \times 10^{14}$ cm^{-2}.

Figure 1 shows the RBS spectra obtained from argon-implanted germanium. The random spectrum results from scattering from a target of randomly distributed atoms since the incident beam enters the crystal at a direction not coinciding with any major crystallographic axes. Therefore, the backscattered yield corresponds to that of an amorphous sample. This spectrum features an edge at 1.767 MeV corresponding to scattering from atoms near the surface, followed by a smoothly increasing yield due to scattering by atoms at greater depths in the crystal. The channeled spectrum of an unimplanted sample is shown for comparison. This undamaged sample exhibits a tenfold decrease in scattering with a small peak in the scattering yield with increasing depth due to dechanneling. Two examples of channeled spectra for ion-damaged samples are also shown in figure 1. The spectrum corresponding to an implanted dose of 1×10^{13} cm^{-2} exhibits a large peak which is due to scattering from atoms displaced from their lattice sites by a length greater than the

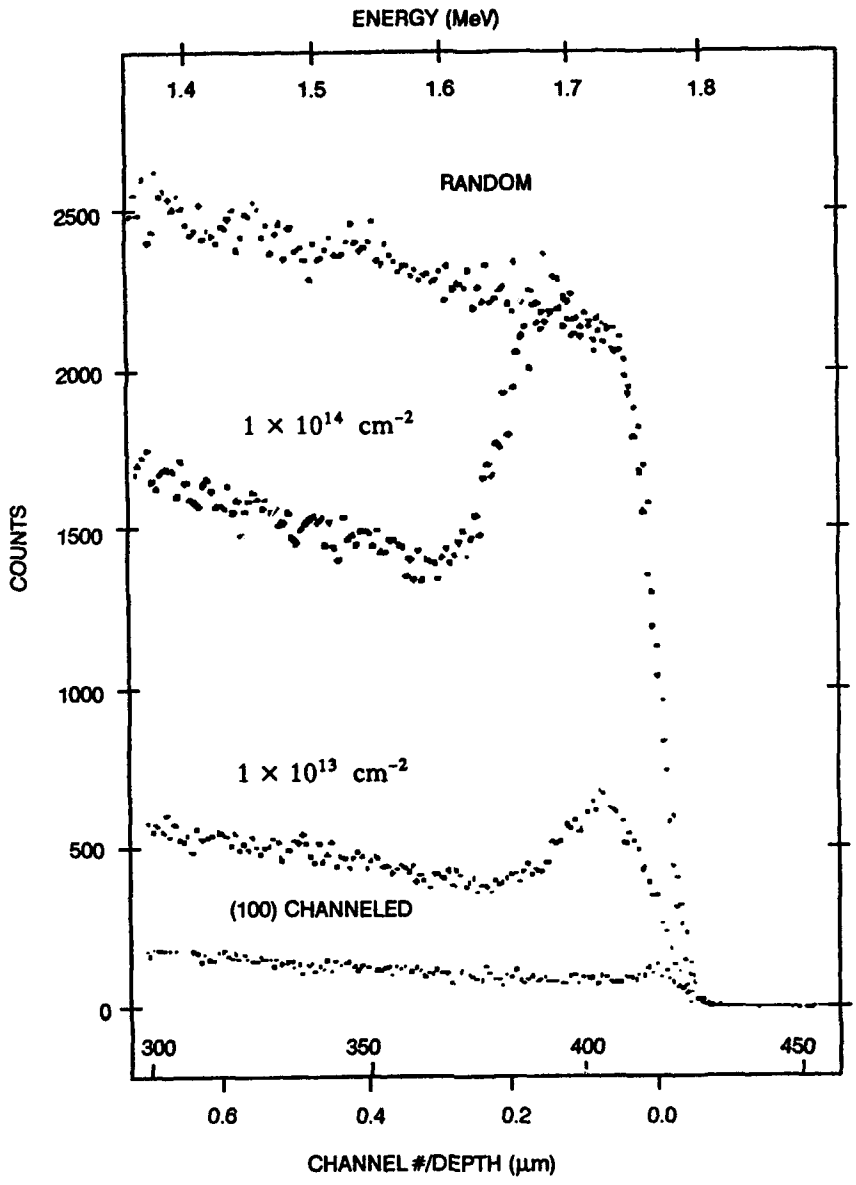

Figure 1. RBS spectra of ion-damaged germanium.

Thomas-Fermi screening length (~0.2 Å in Ge).[30] Upon increasing the dose to 1×10^{14} cm^{-2}, the number of displaced atoms (defects) increases and the scattering yield is comparable to that of the random sample within ~0.2 μm of the surface. Larger doses ($\geq 5 \times 10^{14}$ cm^{-2}) produced a sufficiently large amorphous region such that the dechanneling yield prohibited the attainment of channeled spectra.

The area under the peak in the backscattered yield corrected for dechanneling and surface scattering, is proportional to the amount of damage caused by the implantation. Note, this is greater than the number of displaced atoms since channeling measurements probe disorder in the various defect forms as well as displaced atoms. A summary of our results are shown in figure 2. Here we show the damage as a function of implanted dose, compared with the results of Mayer et. al.[31] At lower doses ($< 10^{14}$ cm^{-2}), the amount of damage increases linearly with increasing dose, which is in agreement with the electron microscopy study of Parsons[32] at oxygen ion doses $< 10^{12}$ cm^{-2}.

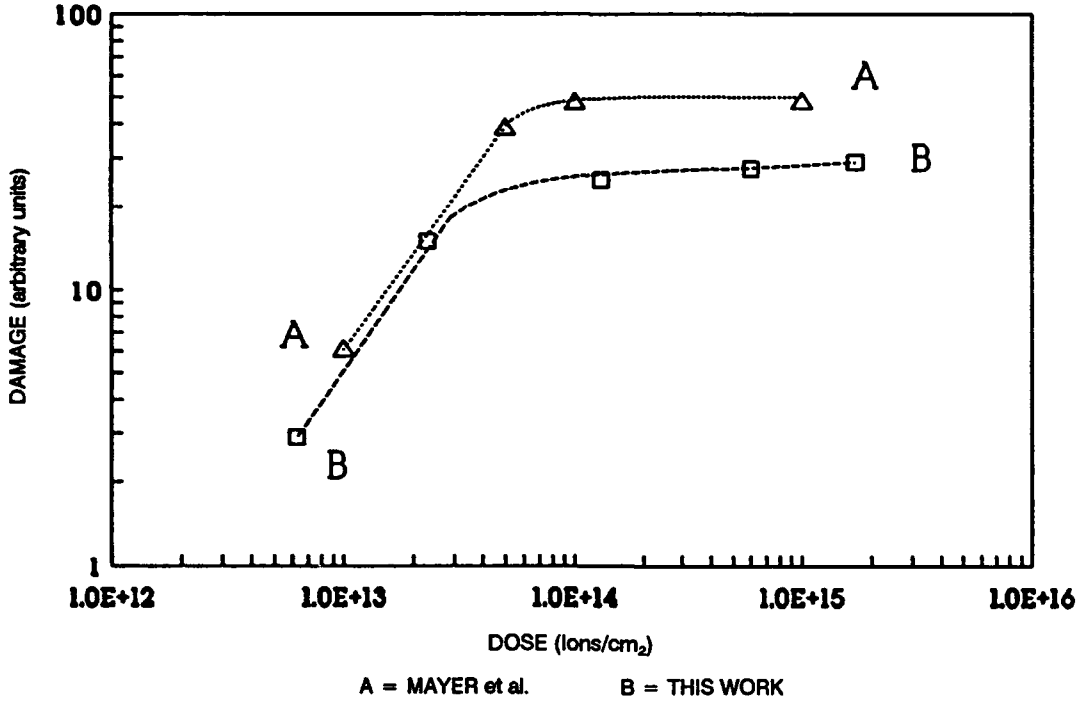

Figure 2. Damage dependence on Ar^+ implantation dose in Ge.

Above the critical dose ($\sim 1 \times 10^{14}$ cm^{-2}), a saturation regime exists. This indicates that at higher doses there is overlapping of the damaged microregions surrounding each ion track (due to cascading collisions) producing an amorphous region. The calculated critical dose of 1.2×10^{14} cm^{-2} agrees extremely well with the experimental results.

Figure 3 shows the damage concentration depth profile extracted from the RBS spectra. This shows that an amorphous region ~ 0.2 μm is produced with a dose of 1×10^{14} cm^{-2}. This agrees with the calculated range for 175 keV argon ions in germanium of 0.13 μm, extending to 0.19 μm including straggle.[33]

4.2 SPREADING RESISTANCE PROFILOMETRY

Figure 4 shows the spreading resistance versus depth for several ion-damaged samples. An undamaged sample (curve A in figure 4), shown for comparison, shows no significant change in R_s with depth. The implanted samples (curves B, C, and D in figure 4) do not show an increase in resistance due to disorder as expected. Instead, we observe the behavior attributed to doping, resulting in the decrease in R_s in the implanted region. With increasing dose, the spreading resistance profile minimum shifts to increasing depths implying that this is not a defect-related signature (since range depends on implant energy and not dose). Based on the results of Appleton et al.[34] and Holland et al.[35], ion implantation can result in adsorption of carbon and oxygen onto the near surface (~ 0.02 μm) of germanium during room temperature implants. This may account for the unexpected resistance behavior. Attempts to activate the suspected impurities by annealing (24 hours at 400°C) proved unsuccessful, with no significant change in spreading resistance profile. The secondary ion mass spectrometry (SIMS) characterization technique would be useful in determining the source of the resistance anomaly, but was not available at this time.

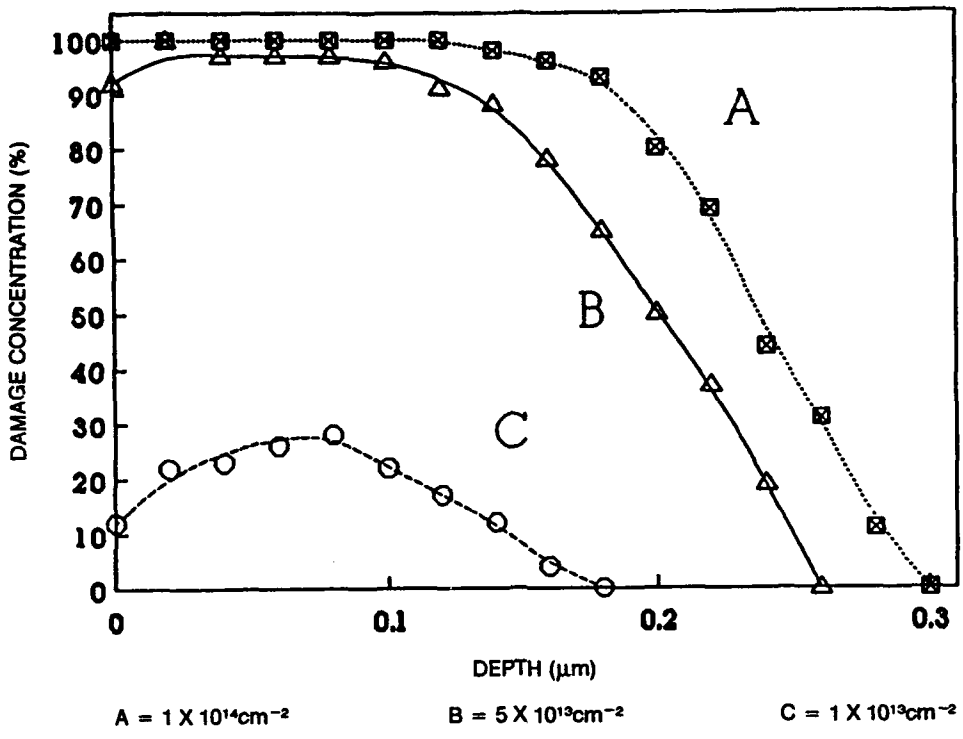

Figure 3. Damage concentration versus depth.

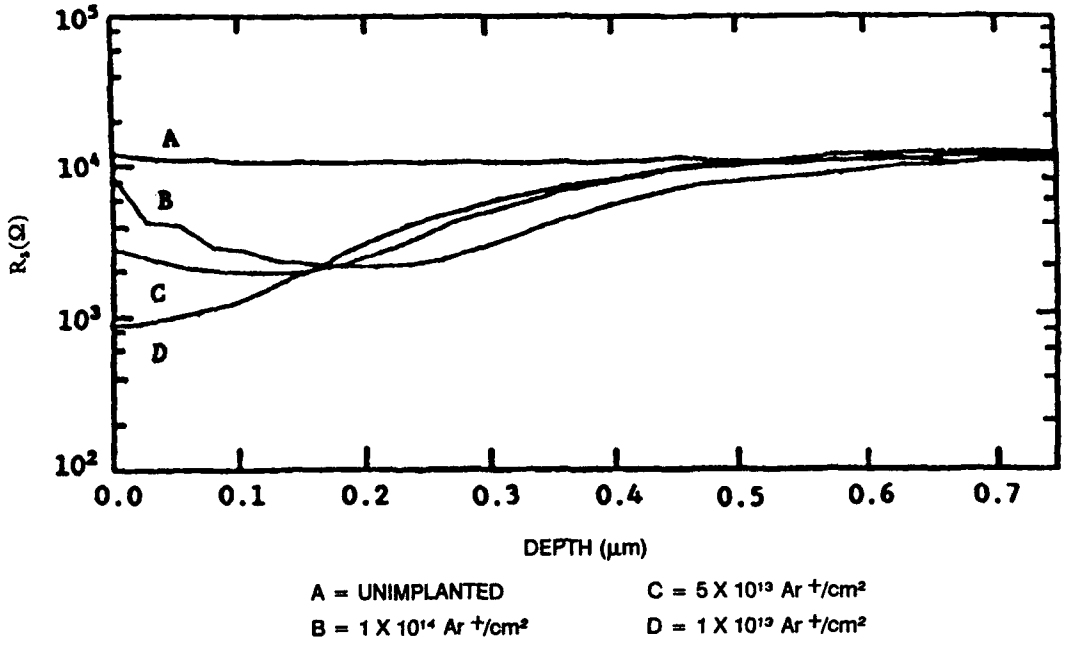

Figure 4. Spreading resistance profile.

4.3 X-RAY DIFFRACTION

X-ray diffraction on damaged and undamaged germanium yielded no significant difference. Transmission Laue photos revealed the principal Bragg reflections in both damaged and undamaged samples, but no evidence of diffuse rings due to disorder were observed. This is due to the small percentage of damaged scattering volume (< 1%) imparted by the implanted ions. Low angle diffractometer scans of Bragg linewidths, or diffraction photos of thinned samples (chemically or via sputtering) are apparent requirements for using this technique in the analysis of damage. Electron diffraction using transmission electron microscopy (TEM) would also require thinned samples to probe only the implanted volume. Reflective high-energy electron diffraction (RHEED) would serve as a useful probe of the disorder due to implantation since it probes only the surface layers.

4.4 PHOTORESPONSE MEASUREMENTS

The photoconductivity (σ) is given by

$$\sigma = Ne\mu \qquad (3)$$

where N is the number of photoinduced charge carriers and μ the electron and hole mobility. The generation of charge carriers (for single photon absorption processes) is proportional to the photon intensity inside the sample.[7] Assuming a quantum efficiency ≈ 1, this implies that the photoconductivity is linear with laser intensity. Resistance measurements on photoexcited undamaged germanium are shown in figure 5. The percentage change in resistance upon laser photoexcitation was used as a relative measure of the photoresponse. Note the linear increase in photoresponse with increasing laser power below ~300 mW. At higher laser intensities, the photoresponse saturates and significant sample heating becomes evident.

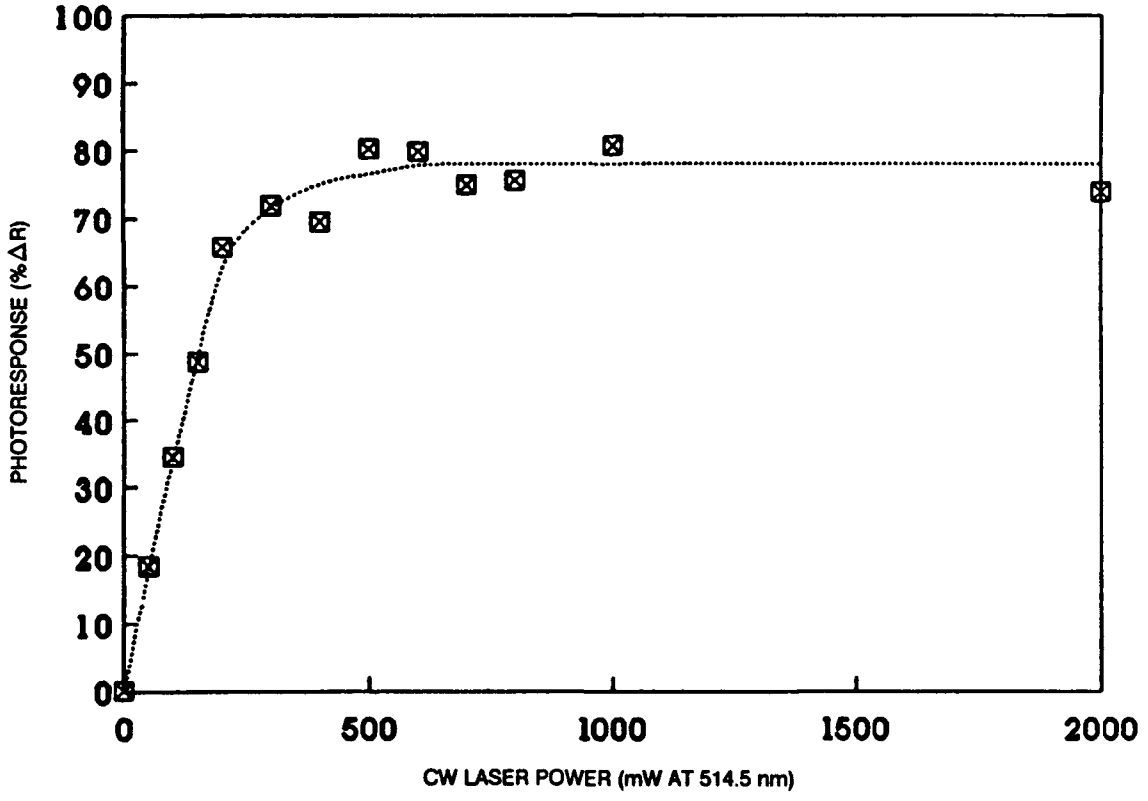

Figure 5. Photoresponse versus laser power for unimplanted Ge.

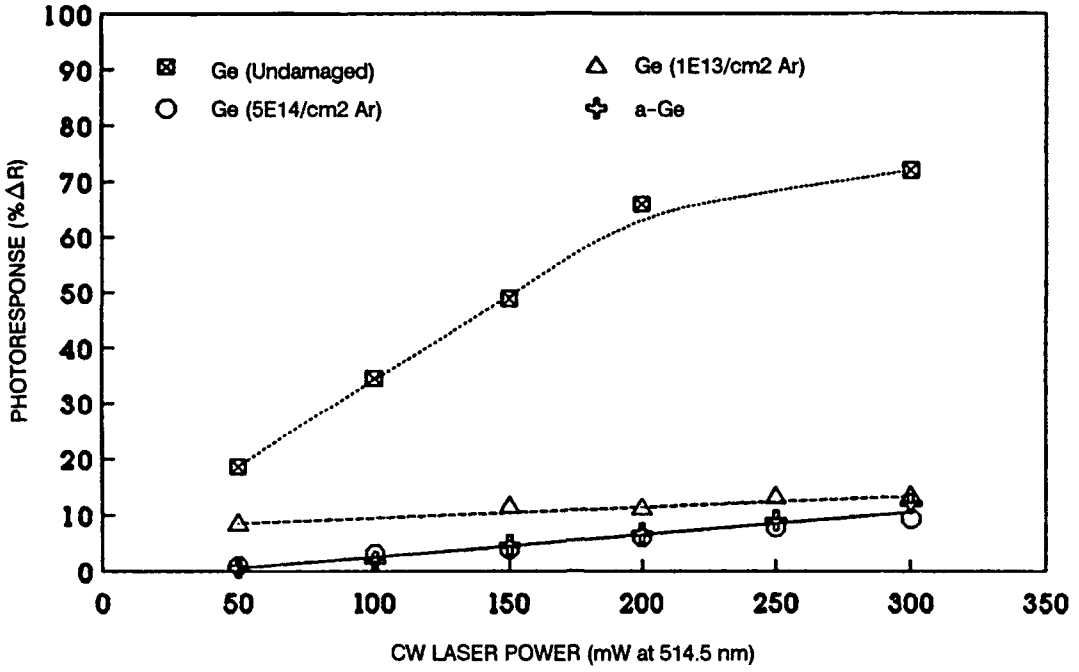

Figure 6. Photoresponse versus laser power from undamaged, moderately damaged (1×10^{13} Ar^+/cm^2), heavily damaged (5×10^{14} Ar^+/cm^2), and amorphous Ge.

Figure 6 compares the photoresponse (in the linear regime) for undamaged, ion-damaged, and amorphous germanium. Small doses of implanted ions ($\sim 1 \times 10^{13}$ cm^{-2}) results in a significant decrease in photoresponsivity compared to the undamaged germanium. Above the critical dose (1×10^{13} cm^{-2}), the samples exhibit similar photoresponse to that of an amorphous sample (consisting of ~5000 Å Ge deposited on (100) p-type Si). This is expected since the absorption coefficient (α) of germanium at 300 K and 5145 Å is 8×10^5 cm^{-1},[5]; therefore the penetration depth ($d_p \approx 0.01$ μm) is less than the depth of the amorphous region in the ion-damaged samples determined by the implanted ion range and straggle (~0.2 μm).

5. CONCLUSION

5.1 SUMMARY

We have determined both theoretically and experimentally the critical dose needed to amorphize germanium using 175 keV argon ions ($D_c \simeq 1 \times 10^{14}$ cm^{-2}). The implantation of ions into germanium can be used to damage samples selectively with predetermined defect densities. Characterization of crystallinity employed x-ray diffraction, spreading resistance profilometry (SRP) and Rutherford backscattering spectroscopy (RBS) techniques. RBS proved to be the most valuable technique in quantifying the degree of damage. Ion-damaged germanium shows a significant decrease in photoresponsivity with implant dose, particularly with doses exceeding the critical amorphizing dose ($D_c \simeq 1 \times 10^{14}$ cm^{-1}). A substantial decrease in photoresponsivity was observed even at low ion doses (1×10^{13} cm^{-2}), therefore, minimizing the degree of damage to achieve the desired switching time will provide the maximum photoresponse for OE switch applications.

5.2 PROPOSED SWITCHING MEASUREMENTS

The switching rate, determined by the recombination rate (U) for a single level recombination process is given by

$$U = \sigma_x v_{th} n_t \cdot \left(\frac{pn - n_i^2}{n + p + 2n_i \cosh\left(\frac{E_t - E_i}{kT}\right)} \right) \quad (4)$$

where σ_x is the electron and hole capture cross section (assuming $\sigma_e = \sigma_n = \sigma_x$), v_{th} the carrier thermal velocity, with n_i and n_t the intrinsic and trap densities and E_i the intrinsic fermi level.[2] The recombination rate (U) is therefore linear in trap density (n_t); however, not all traps will play a major role in the OE switch operation. Dislocations in as-grown germanium crystals act as electrical traps at sufficiently high concentrations.[36,37] In p-type Ge, dislocations along the (112) direction have a trapping level at E_v + 25 meV.[38] The dominant defects in determining the recombination rate are however the vacancies (and divacancies) imparted by ion implantation and not dislocations due to trapping energies closer to midgap (as seen from equation 4). Measurements into the switching rate as a function of implant dose (i.e., damage) were planned for these characterized samples. Early attempts at switch fabrication using standard photolithography techniques have proved unsuccessful. Both deposition and sputtering techniques were used in constructing aluminum (Al) electrodes ≈1500 Å in thickness on samples that had been degreased and cleaned as described earlier, and dehydrated at 135°C for 1 hour. Subsequent processing resulted in loss of adhesion of the electrode to the sample surface. Whereas DeFonzo (1981)[13] used aluminum and an aluminum-gold alloy for microstrip fabrication on OE switches successfully, Marshall et al. (1985), note that Al contacts with germanium do not become ohmic at annealing temperatures (230°C to 800°C for 30 minutes) and maintain a Schottky barrier of ϕ_b = 0.63 eV.[39] Solutions to these contact problems need to be developed before OE switches can be fabricated on germanium. Then the optimal implant dose required for satisfactory switching times can be determined.

5.3 OTHER DIRECTIONS

The ion-implantation technique has proven to be effective in controlling material structure and thereby its electrical and photoconductive characteristics. Future control using focused ion beams for implanting may be used for spatial control now lacking in the technique. Implantation into the interelectrode gap on OE switches would presumably decrease the recombination time while maintaining the overall photoresponsivity of the switch, effectively decoupling this aforementioned "tradeoff." This has been attained by DeFonzo (1981)[13] using laser recrystallization without the control of damage available with implantation.

Recent growth of Ge_xSi_{1-x} alloy films on silicon[40-43] present another avenue for OE switch material. Deposition of germanium films on silicon results in a large number of defects at the interface (clearly observed with RBS) due to the lattice mismatch. Alloy growth techniques will enable the growth of epitaxial germanium on silicon using a gradient alloy layer to mediate the lattice mismatch. In addition, the control of alloy composition will enable the tuning of the bandgap for various device applications, which is a technique used on $Al_xGa_{1-x}As$ technology. Research in Ge_xSi_{1-x} alloy fabrication using excimer laser mixing are being initiated in collaboration with Dr. D. A. Sexton, NOSC Code 554. Successful efforts using this technology to fabricate photodetectors may incorporate the ion-damaged techniques investigated here.

Advances in materials growth have led to semiconductor heterostructures composed of superlattices of ultrathin n- and p-doped layers with intrinsic layers of the same material in between, so-called "nipi crystals". Nipi structures of amorphous (hydrogenated) silicon (a-Si:H) have been produced, and show a tenfold increase in their infrared (IR) photoconductivity compared to unstructured a-Si:H.[44] Extensions to germanium and Ge/Si alloys seem a viable direction for research as well.

6. GLOSSARY

Å	angstrom
Al	aluminum
Ar	argon
a-Si	amorphous silicon
C	celcius
cm	centimeter
Cr	chromium
cw	continuous wave
eV	electron volts
Fe	iron
GaAs	gallium arsenide
Ge	germanium
He	helium
InP	indium phosphide
K	kelvin
keV	kiloelectron volts
μA	microampere
μm	micrometer
MeV	megaelectron volts
mrads	milliradian
mW	milliwatt
MSM	metal-semiconductor metal
nm	nanometer
OE	optoelectronics
p-Ge	polycrystalline germanium
ps	picosecond
RBS	Rutherford backscattering (technique)
RHEED	reflective high-energy electron diffraction
rms	root mean square
SIMS	secondary ion mass spectrometry
SOS	silicon-on-sapphire
SRP	spreading resistance profilometry
TDM	time division multiplexing
TEM	transmission electron microscopy
VHSIC	very-high-speed integrated circuits
VLSI	very-large-scale integration

7. REFERENCES

1. Albares, D. J., and R. E. Reedy. September 1984. "Optical Techniques for Advanced VLSI/VHSIC Interconnections." NOSC TR984 Naval Ocean Systems Center, San Diego, CA.

2. Sze, S. M. 1981. *Physics of Semiconductor Devices*, John Wiley & Sons, NY.

3. Albares, D. J., G. A. Garcia, C. T. Chang, and R. E. Reedy. 1987. "Optoelectronic Time Division Multiplexing," *Electron. Lett., 23*, p. 327.

4. Albares, D. J., G. A. Garcia, G. P. Imthurn, T. R. Ogden, M. J. Taylor, and C. T. Chang. 1989. "Optoelectronic Time Division Multiplexing for Computer Interconnections," in R. R. Chen, ed., *Twenty-third Asilomar Conference on Signals, Systems & Computers, Conference Record*, vol. 1, IEEE Computer Society, San Jose, CA: Maple Press, Inc., p. 89.

5. Hogarth, C. A., ed. 1965. *Materials Used in Semiconductor Devices*, Interscience Publishers, NY.

6. Dash, W. C., and R. Newman. 1955. "Intrinsic Optical Absorption in Single-Crystal Germanium and Silicon at 77 K and 300 K," *Phys. Rev., 99*, p. 1151.

7. Lee, C. H., ed. 1984. *Picosecond Optoelectronic Devices*, Academic Press, SD.

8. Smith, P. R., D. H. Auston, A. M. Johnson, and W. M. Augustyniak. 1981. "Picosecond Photoconductivity in Radiation Damaged Silicon-on-Sapphire Films," *Appl. Phys. Lett., 38*, p. 47 *and references therein.*

9. Foyt, A. G., F. J. Leonberger, and R. C. Williamson. 1982. "Picosecond InP Optoelectronic Switches," *Appl. Phys. Lett., 40*, p. 447 *and references therein.*

10. Bergner, H., V. Brucker, F. Kerstan, and W. Nowick. 1985. "Picosecond Processes of Laser-Excited Carriers in Silicon on Sapphire," *Phys. Stat. Sol. (B), 128*, p. 769 *and references therein.*

11. Auston, D. H., P. Lavallard, N. Sol, and D. Kaplan. 1980. "An Amorphous Silicon Photodetector for Picosecond Pulses," *Appl. Phys. Lett., 36*, p. 66.

12. Foyt, A. G., F. J. Leonberger, and R. C. Williamson. 1981. "InP Optoelectronic Mixers," *Integrated Optics, Proc. SPIE, 269*, p. 109.

13. DeFonzo, A. P. 1981. "Picosecond Photoconductivity in Germanium Films," *Appl. Phys. Lett., 39*, p. 480.

14. Auston, D. H., A. M. Johnson, P. R. Smith, and J. C. Bean. 1980. "Picosecond Optoelectronic Detection, Sampling, and Correlation Measurements in Amorphous Semiconductors," *Appl. Phys. Lett., 37*, p. 371.

15. Johnson, A. M., D. H. Auston, P. R. Smith, J. C. Bean, J. P. Harbison, and A. C. Adams. 1981. "Picosecond Transient Photocurrents in Amorphous Silicon," *Phys. Rev. B, 23*, p. 6816.

16. Lax, M. 1960. "Cascade Capture of Electrons in Solids," *Phys. Rev., 119*, p. 1502.

17. Stockman, F. 1917. "Recombination Kinetics in Photoconductors," in E. M. Pell, ed., *Proc of the 3rd Intl Conf on Photoconductivity*, Pergamon Press, NY, p. 17 *and references therein.*

18. Gershenzon, E. M., G. N. Gol'tsman, V. V. Multanovskii, and N. G. Ptitsyna. 1979. "Capture of Photoexcited Carriers by Shallow Impurity Centers in Germanium," *Sov. Phys. JETP, 50*, p. 728, [*Zh. Eksp. Teor. Fiz., 77*, p. 1450, 1982].

19. Gershenzon, E. M., G. N. Gol'tsman, V. V. Multanovskii, and N. G. Ptitsina (sic). 1982. "Kinetics of Submillimeter Impurity and Exciton Photoconduction in Ge," *Opt. Spectrosc (USSR), 52*, p. 454, [*Opt. Spektrosk, 52*, p. 756, 1982].

20. Bergner, H., V. Bruckner, and B. Schroder. 1983. "Investigation of Fast Processes in Semiconductors in the Picosecond Range," *Sov. J. Quantum Electron., 13*, p. 736, [*Kuantovaya Elektron (Moscow), 10*, p. 1150, 1983].

21. Ashkinadze, B. M., and N. R. Tevs. 1985. "Temperature Dependence of the Lifetime in Pure Germanium," *Sov. Phys. Semicond. 19*, p. 688, [*Fiz. Tekh. Poluprovodn., 19*, p. 1122, 1985].

22. Bergner, H., V. Bruckner, F. Kerstan, and W. Nowick. 1983. "Comparative Studies of Fast Recombination Processes in Amorphous Silicon Films," *Phys. Stat. Sol. (B), 117*, p. 603.

23. Leonberger, F. J., and P. F. Moulton. 1979. "High Speed InP Optoelectronic Switch," *Appl. Phys. Lett., 35*, p. 712.

24. Bruckner, V., and F. Kerstan. 1984. "Optoelectronic Switches Made of Semiconductors," *Sov. J. Quantum Elektron., 14*, p. 909, [*Kvantovaya Elektron (Moscow), 11*, p. 1344, 1984].

25. Kappert, H. F., G. Sixt, and G. H. Schwuttke. 1979. "Minority Carrier Lifetime in Silicon After Ar^+ and Si^+ Implantation," *Phys. Stat. Sol. (A), 52*, p. 463.

26. Chu, W. K., J. W. Mayer, and M. A. Nicolet. 1978. *Backscattering Spectrometry*, Academic Press, San Francisco, CA.

27. *Coherent Supergraphite Series Ion Laser Manual.* 1978. Coherent, Palo Alto, CA.

28. Kagawa, S., T. Mikawa, and T. Kaneda. 1982. "Chemical Etching of Germanium with H_3PO_4 - H_2O_2 - H_2O Solution," *Jpn. J. Appl. Phys. Part 1, 21*, p. 1616.

29. Morehead, Jr., F. F., and B. L. Crowder. 1971. "A Model for the Formation of Amorphous Si by Ion Bombardment," in F.H. Eisen, L. T. Chadderton, eds., *Ion Implantation*, Gordon and Breach Science Publishers, NY, p. 25.

30. Mayer, J. W., L. Eriksson, and J. A. Davies. 1970. *Ion Implantation in Semiconductors*, Academic Press, NY.

31. Mayer, J. W., E. Eriksson, S. T. Picraux, and J. A. Davies. 1968. "Ion Implantation of Silicon and Germanium at Room Temperature. Analysis by Means of 1.0 MeV Helium Ion Scattering," *Can. J. Chem., 46*, p. 663.

32. Parsons, J. R. 1965. "Conversion of Crystalline Germanium to Amorphous Germanium by Ion Bombardment," *Phil. Mag., 12*, p. 1159.

33. Ziegler, J. F., J. P. Biersack, and V. Littmark. 1985. Range Calculations Performed Using the Software "TRIM-86", version 2.0, from *The Stopping Range of Ions in Matter*, Pergamon Press, NY.

34. Appleton, B. R., O. W. Holland, J. Narayan, O. E. Schow III, J. S. Williams, K. T. Short, and E. Lawson. 1982. "Characterization of Damage in Ion Implanted Ge," *Appl. Phys, Lett., 41*, p. 711.

35. Holland, O. W., B. R. Appleton, and J. Narayan. 1983. "Ion Implantation Damage and Annealing in Germanium," *J. Appl. Phys., 54*, p. 2295.

36. Glasow, P. A., and E. E. Haller. 1976. "The Effect of Dislocations on the Energy Resolution of High-Purity Germanium Detectors," *IEEE Trans. Nucl. Sci., NS-23*, p. 92.

37. Simoen, E., P. Clauws, J. Broeckx, J. Vennik, M. Van Sande, and L. De Laet. 1982. "Correlation Between DLTS-Measurements and the Performance of High-Purity Germanium Detectors," *IEEE Trans. Nucl. Sci., NS-29*, p. 789.

38. Van Sande, M., L. Van Goethem, L. De Laet, and H. Guislain. 1986. "Dislocations in High-Purity Germanium and Its Relation to X-Ray Detector Performance," *Appl. Phys. A, 40*, p. 257.

39. Marshall, E. D., C. S. Wu, C. S. Pai, D. M. Scott, and S. S. Lau. 1985. "Metal-Germanium Contacts and Germinide Formation," *Mat. Res. Soc. Symp. Proc.*, vol. 47, *Materials Research Society*, p. 161.

40. Fan, J. C. C., R. P. Gale, and G. H. Foley. 1980. "Heteroepitaxy of $Ge_{1-x}Si_x$ on Si by Transient Heating of Ge-Coated Si Substrates," *Appl. Phys. Lett., 37*, p. 1024.

41. Luryi, S., A. Kastralsky, and J. C. Bean. 1984. "New Infrared Detector on a Silicon Chip," *IEEE Trans. El. Dev., ED-31*, p. 1135.

42. Bean, J. C., T. T. Sheng, L. C. Feldman, A. T. Fiory, and R. T. Lynch. 1984. "Pseudomorphic Growth of Ge_xSi_{1-x} on Silicon by Molecular Beam Epitaxy," *Appl. Phys. Lett., 44*, p. 102.

43. Bean, J. C. October 1986. "The Growth of Novel Silicon Materials," *Physics Today*, vol. 39, no. 10, p. 36.

44. Hundhausen, M., L. Ley, and R. Carius. 1984. "Carrier Recombination Times in Amorphous-Silicon Doping Superlattices," *Phys. Rev. Lett., 53*, p. 1598.

REPORT DOCUMENTATION PAGE

Form Approved
OMB No. 0704-0188

1. AGENCY USE ONLY *(Leave blank)*	2. REPORT DATE	3. REPORT TYPE AND DATES COVERED
	December 1990	Final: June 1986 – October 1986

4. TITLE AND SUBTITLE

PHOTORESPONSE STUDIES OF ION-DAMAGED GERMANIUM FOR OPTOELECTRONIC SWITCH APPLICATIONS

5. FUNDING NUMBERS

PE: 0602301E
SUBPROJ: 55-EE8701
ACC: DN388650

6. AUTHOR(S)

S. D. Russell

7. PERFORMING ORGANIZATION NAME(S) AND ADDRESS(ES)

Naval Ocean Systems Center
Code 553
San Diego, CA 92152–5000

8. PERFORMING ORGANIZATION REPORT NUMBER

NOSC TD 1963

9. SPONSORING/MONITORING AGENCY NAME(S) AND ADDRESS(ES)

Defense Advanced Projects Agency
(DARPA-NA)
1400 Wilson Boulevard
Arlington, VA 22209

10. SPONSORING/MONITORING AGENCY REPORT NUMBER

11. SUPPLEMENTARY NOTES

12a. DISTRIBUTION/AVAILABILITY STATEMENT

Approved for public release; distribution is unlimited.

12b. DISTRIBUTION CODE

13. ABSTRACT *(Maximum 200 words)*

In light of the potential of germanium optoelectronic (OE) switches for OE/time division multiplexing (OE/TDM) applications, preliminary research into the effect of crystalline damage on its photoresponse was performed. This document reports the results of this proposed method to decrease the photocurrent decay time for high-speed OE switches.

14. SUBJECT TERMS

optoelectronic switch, germanium (Ge), Rutherford backscattering (RBS), very-high-speed integrated circuits (VHSIC), amorphous silicon (a-Si), silicon-on-sapphire (SOS), polycrystalline germanium (p-Ge), photoconductivity, chemical vapor deposition (CVD)

15. NUMBER OF PAGES

19

16. PRICE CODE

17. SECURITY CLASSIFICATION OF REPORT	18. SECURITY CLASSIFICATION OF THIS PAGE	19. SECURITY CLASSIFICATION OF ABSTRACT	20. LIMITATION OF ABSTRACT
UNCLASSIFIED	UNCLASSIFIED	UNCLASSIFIED	SAME AS REPORT

INITIAL DISTRIBUTION

CODE 0012	Patent Counsel	(1)
CODE 0144	R. November	(1)
CODE 55	H. E. Rast	(1)
CODE 553	S. D. Russell	(15)
CODE 553	D. J. Albares	(2)
CODE 553	G. A. Garcia	(1)
CODE 554	E. P. Kelley	(1)
CODE 554	D. A. Sexton	(1)
CODE 921	J. Puleo	(1)
CODE 961	Archive/Stock	(6)
CODE 964	Library	(3)

Defense Technical Information Center
Alexandria, VA 22304-6145 (4)

NOSC Liaison Office
Washington, DC 20363-5100 (1)

Center for Naval Analyses
Alexandria, VA 22302-0268 (1)